


# Structural and Hirshfeld Surface Analyses of a Novel Hetero-Tetranuclear $\text{Cu}^{\text{II}}\text{-Na}^{\text{I}}$ Bis(Salamo)-Based Coordination Compound

Ya-Xuan Sun <sup>1</sup>, Ling-Zhi Liu <sup>2</sup>, Fei Wang <sup>2</sup>, Xiao-Ya Shang <sup>1,\*</sup>, Le Chen <sup>2</sup> and Wen-Kui Dong <sup>2,\*</sup> 

<sup>1</sup> Beijing Key Laboratory of Bioactive Substances and Functional Foods, Beijing Union University, Beijing 100191, China; sunxx@bnu.edu.cn

<sup>2</sup> School of Chemical and Biological Engineering, Lanzhou Jiaotong University, Lanzhou 730070, China; llz1009663202@126.com (L.-Z.L.); wangfei3986@163.com (F.W.); chenle405@163.com (L.C.)

\* Correspondence: shangxiaoya@bnu.edu.cn (X.-Y.S.); dongwk@126.com (W.-K.D.); Tel.: +86-931-493-8703 (W.-K.D.)

Received: 12 March 2018; Accepted: 16 May 2018; Published: 18 May 2018



**Abstract:** The newly designed butterfly-shaped hetero-tetranuclear  $\text{Cu}^{\text{II}}\text{-Na}^{\text{I}}$  coordination compound,  $[\text{Cu}_3(\text{HL})_2\text{Na}]\cdot\text{Pic}$  (Pic<sup>−</sup> is abbreviation of picrate) (**1**) which is derived from a naphthalenediol-based bis(Salamo)-type chelating ligand  $\text{H}_4\text{L}$  have been synthesized and characterized by elemental analyses, UV-vis spectra, IR spectra analysis, and Hirshfeld surface analysis. X-ray crystallographic analyses revealed that the coordination compound **1** is a novel hetero-tetranuclear  $\text{Cu}^{\text{II}}\text{-Na}^{\text{I}}$  bis(Salamo)-type coordination compound and it differs from heterotrinuclear  $\text{Cu}^{\text{II}}\text{-Na}^{\text{I}}$  bis(Salamo)-type coordination compound reported earlier. The Cu1 and Cu3 atoms are tetra-coordinated with geometries of distorted square pyramid, while Cu2 atom are hexa-coordinated with the geometry of a distorted octahedron. The  $\text{Na}^{\text{I}}$  atom is octa-coordinated with the geometry of a distorted hexagonal bipyramid. Furthermore, the supramolecular structure and Hirshfeld surface analyses have been discussed in detail.

**Keywords:** bis(Salamo)-type ligand; hetero-tetranuclear;  $\text{Cu}^{\text{II}}\text{-Na}^{\text{I}}$  coordination compound; crystal structure; hirshfeld surface analysis

## 1. Introduction

Salen-type ligands and their coordination compounds have been extensively investigated [1–10] for their catalytic activities [11–15], biological activities [16–22], supramolecular architectures [23–32], and fluorescence properties [33–38]. To improve the properties of Salen-type ligands, in recent years, Nabeshima and our group's researches mostly concentrated on the syntheses of Salamo-type ligands, which are a class of novel Salen-type analogues [39–51]. These Salamo-type multidentate ligands can self-assemble with transition metals, alkali metals, alkaline earth metals, and rare earth metals to form mononuclear or multinuclear 3d, 3d-s, 3d-4f coordination compounds [52–60]. Furthermore, these coordination compounds exhibit unique fluorescent and magnetic properties [61,62], anion effects [63], and ions recognitions [64,65], based on their structural characteristics. Meanwhile, supramolecular chemistry has become increasingly prominent in the coordination chemistry, for Salamo-type metal coordination compounds, supramolecular structures are formed mainly with the help of C–H $\cdots$ O, C–H $\cdots$  $\pi$  or  $\pi\cdots\pi$  interactions [66–68]. Bis(Salamo)-type ligands and their complexes have also been explored by the Nabeshima group [69–73], however, the heteropolynuclear  $\text{Cu}^{\text{II}}\text{-Na}^{\text{I}}$  bis(Salamo)-type coordination compounds were rarely reported [74].

Recently, our research project concentrated on the syntheses of a new naphthalenediol-based bis(Salamo)-type ligands  $\text{H}_4\text{L}$  containing two Salamo  $\text{N}_2\text{O}_2$  chelate moieties and their corresponding

homo- or hetero-polynuclear metal coordination compounds, which differ from Nabeshima group's research emphasis. Herein, in order to study the anion effect of coordination compounds, we have designed and synthesized a novel  $\text{Cu}^{\text{II}}\text{-Na}^{\text{I}}$  coordination compound  $[\text{Cu}_3(\text{HL})_2\text{Na}]\cdot\text{Pic}$ , which is different from our previously reported coordination compound  $[\text{Cu}_2(\text{L})\text{Na}(\text{NO}_3)(\text{CH}_3\text{OH})]$  [74].

## 2. Experimental

### 2.1. Materials and Methods

All of the chemical reagents are analytical pure reagents, which have not been purified before being used. C, H, and N analyses were obtained using a GmbH VarioEL V3.00 automatic elemental analyzer (Berlin, Germany). Elemental analysis for copper was detected by IRIS ER/S-WP-1 ICP atomic emission spectrometer (Elementar, Berlin, Germany). The melting points were determined by microscopic melting point instrument made in Beijing Tektronix Instruments Limited Company.  $^1\text{H-NMR}$  spectra were recorded by German Bruker AVANCE DRX-400 spectroscopy (Bruker AVANCE, Billerica, MA, USA). Infrared spectra were measured with a VERTEX-70 FT-IR spectrophotometer (Bruker, Billerica, MA, USA), with samples that were prepared as KBr ( $400\text{--}4000\text{ cm}^{-1}$ ). UV/Vis absorption spectra were recorded on a Shimadzu UV-2550 spectrometer (Shimadzu, Tokyo, Japan). X-ray single crystal structure determination was carried out on a Bruker Smart Apex CCD diffractometer (Bruker AVANCE, Billerica, MA, USA).

### 2.2. Synthesis of $\text{H}_4\text{L}$

A naphthalenediol-based bis(Salamo)-type ligand ( $\text{H}_4\text{L}$ ) was synthesized according to the procedure reported earlier [11,74]. Yield: 85%. Mp  $205\text{--}207\text{ }^\circ\text{C}$ . Anal. Calcd for  $\text{C}_{30}\text{H}_{24}\text{Br}_4\text{N}_4\text{O}_8$  (%): C, 40.57; H, 2.72; N, 6.31. Found: C, 40.74; H, 2.70; N, 6.18.  $^1\text{H-NMR}$  (400 MHz,  $\text{DMSO-d}_6$ , 298 K):  $\delta = 4.56$  (s, 8H;  $\text{OCH-H}$ ), 7.38–7.40 (m, 2H;  $\text{Ar-H}$ ), 7.69 (s, 2H;  $\text{Ar-H}$ ), 7.81 (s, 2H;  $\text{Ar-H}$ ), 8.47–8.49 (m, 2H;  $\text{Ar-H}$ ), 8.51 (s, 2H;  $\text{N=C-H}$ ), 9.10 (s, 2H;  $\text{N=C-H}$ ), and 10.59 (s, 4H;  $\text{O-H}$ ).

### 2.3. Synthesis of the Coordination Compound 1

A chloroform solution (3.0 mL) of copper(II) picrate tetrahydrate (0.015 mmol, 8.84 mg) was added dropwise to the mixture solution of  $\text{H}_4\text{L}$  (0.01 mmol, 8.80 mg) and NaOH (0.80 mg, 0.020 mmol) in methanol (3.0 mL) at room temperature, and the color changed to dark brown immediately. The mixture was filtered and the filtrate was allowed to stand at room temperature for about two weeks. The solvent was partially evaporated and brown block crystals suitable for X-ray crystallographic analysis were obtained. Yield: 5.21 mg, 47.1%. Anal. Calcd for  $\text{C}_{66}\text{H}_{44}\text{Br}_8\text{Cu}_3\text{NaN}_{11}\text{O}_{23}$  (%): C, 35.84; H, 2.00; N, 6.97; Cu, 8.62. Found: C, 36.01; H, 1.89; N, 6.87; and, Cu, 8.51.

### 2.4. Crystal Structure Determinations of the Coordination Compound 1

A crystal diffractometer provides a monochromatic beam of Mo  $\text{K}\alpha$  radiation ( $0.71073\text{ \AA}$ ) that was produced from a sealed Mo X-ray tube using a graphite monochromator and was used for obtaining crystal data for the coordination compound 1 at 291 (2) K. The LP factor and semi-empirical absorption corrections were applied using the SADABS program. The structure was solved by the direct methods (SHELXS-2016) [75]. All of the hydrogen atoms were added theoretically and a difference-Fourier map revealed the positions of the remaining atoms. All non-hydrogen atoms were refined anisotropically using a full-matrix least-squares procedure on  $F^2$  with SHELXL-2016 [76]. The crystal data and experimental parameters of the coordination compound 1 are summarized in Table 1. Supplementary crystallographic data for this paper have been deposited at Cambridge Crystallographic Data Centre (1828273) and can be obtained free of charge via [www.ccdc.cam.ac.uk/conts/retrieving.html](http://www.ccdc.cam.ac.uk/conts/retrieving.html).

**Table 1.** Crystal data and structure refinement parameters for the coordination compound **1**.

Coordination Compound	[Cu <sub>3</sub> (HL) <sub>2</sub> Na]·Pic
Formula	C <sub>66</sub> H <sub>44</sub> Br <sub>8</sub> Cu <sub>3</sub> NaN <sub>11</sub> O <sub>23</sub>
Formula weight	2212.01
Temperature (K)	291(2)
Wavelength (Å)	0.71073
Crystal system	Monoclinic
Space group	<i>P</i> 2 <sub>1</sub> / <i>n</i>
Unit cell dimensions	
<i>a</i> (Å)	15.6350(14)
<i>b</i> (Å)	18.2157(18)
<i>c</i> (Å)	28.691(3)
α (°)	90
β (°)	91.787(3)
γ (°)	90
<i>V</i> (Å <sup>3</sup> )	1006.90(19)
<i>Z</i>	4
<i>D<sub>c</sub></i> (g cm <sup>−3</sup> )	1.799
μ (mm <sup>−1</sup> )	4.771
<i>F</i> (000)	4316
Crystal size (mm)	0.24 × 0.22 × 0.20
θ Range (°)	2.2360–27.5520
Index ranges	−20 ≤ <i>h</i> ≤ 20, −23 ≤ <i>k</i> ≤ 16, −36 ≤ <i>l</i> ≤ 37
Reflections collected	46,887
Independent reflections	18,150
<i>R</i> <sub>int</sub>	0.0257
Completeness	97.5%
Data/restraints/parameters	18150/7/1010
GOF	1.062
Final <i>R</i> <sub>1</sub> , <i>wR</i> <sub>2</sub> indices [ <i>I</i> > 2σ( <i>I</i> )]	0.0571/0.1266
<i>R</i> <sub>1</sub> , <i>wR</i> <sub>2</sub> indices (all data)	0.0949/0.1350

$$R_1 = \sum ||F_o| - |F_c|| / \sum |F_o|; wR_2 = \{\sum w(F_o^2 - F_c^2)^2 / \sum [w(F_o^2)]^2\}^{1/2}.$$

### 3. Results and Discussion

#### 3.1. Crystal Structure of the Coordination Compound **1**

The crystal structure and atom numbering of the coordination compound **1** are shown in Figure 1. Selected major bond lengths and angles are listed in Table 2.

The crystallographic data revealed that the coordination compound **1** crystallizes in the monoclinic system, space group *P*2<sub>1</sub>/*n*. X-ray crystallography clearly showed that the coordination compound **1** is a hetero-tetranuclear butterfly-shape coordination compound, which consists of two deprotonated (HL)<sup>3−</sup> units, three Cu<sup>II</sup> atoms, one Na<sup>I</sup> atom, and one uncoordinated picrate ion. Note worthily, this 2:3 ((HL)<sup>3−</sup>:Cu<sup>II</sup>) type hetero-tetranuclear Cu<sup>II</sup>-Na<sup>I</sup> coordination compound is different from the earlier reported Cu<sup>II</sup> Salamo-type coordination compounds of 1:2 [77–79], 2:2 [80–82], 2:3 [83], and 2:4 [83] type (L:Cu<sup>II</sup>). Especially, this is the first bis(Salamo)-based metal complex containing two bis(Salamo)-type ligands. The coordination compound that is obtained is different from our previously reported coordination compound [Cu<sub>2</sub>(L)Na(NO<sub>3</sub>)(CH<sub>3</sub>OH)], in which the two Cu(II) atoms are located in N<sub>2</sub>O<sub>2</sub> cavities, and one Cu(II) atom is still bonded to a methanol molecule, while the other Cu(II) atom is coordinated with one oxygen atom of a μ<sub>3</sub>-NO<sub>3</sub> ion. Finally, both Cu(II) atoms adopt penta-coordinated with geometries of slightly distorted tetragonal pyramid [74].

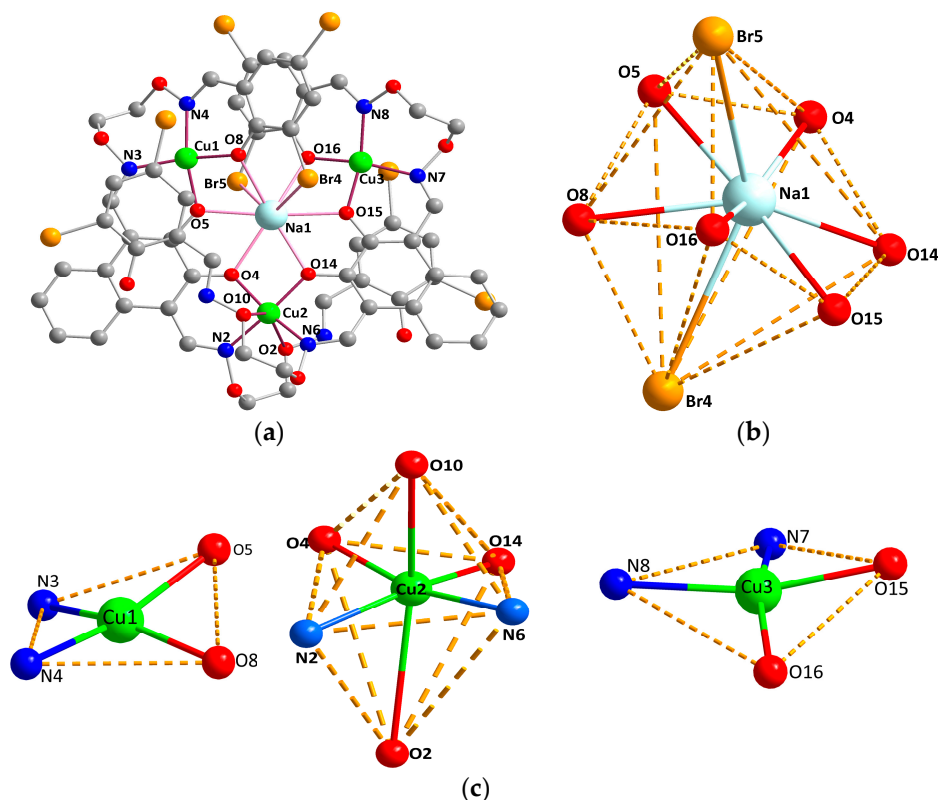


**Figure 1.** (a) Molecular structure and atom numberings of the coordination compound **1** (hydrogen atoms are omitted for clarity); (b) Coordination polyhedron for the Na<sup>I</sup> atom of the coordination compound **1**; and, (c) Coordination polyhedrons for Cu<sup>II</sup> atoms of the coordination compound **1**.

**Table 2.** Selected bond lengths (Å) and angles (°) for the coordination compound **1**.

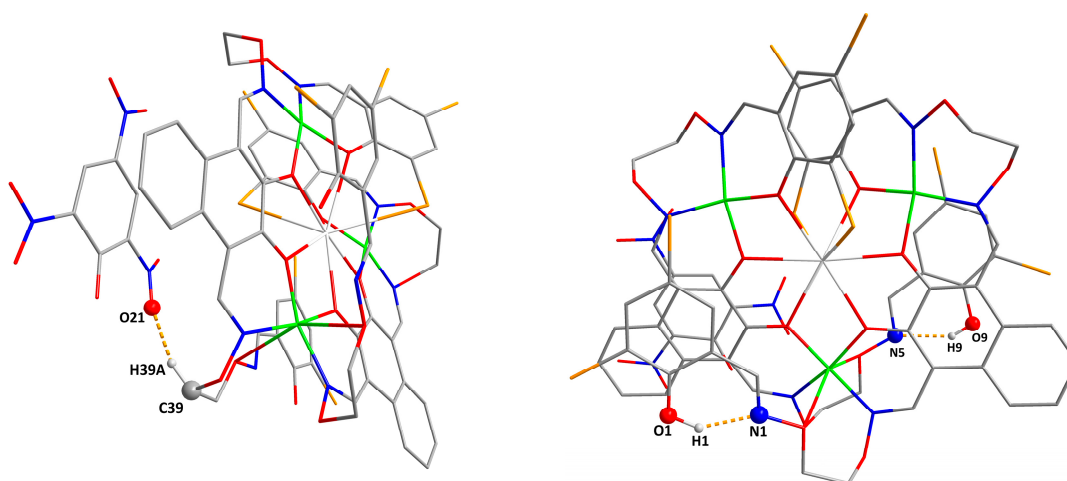
Bond		Bond	
Cu1-O5	1.888(3)	Cu3-O16	1.900(3)
Cu1-O8	1.901(3)	Cu3-N7	1.936(4)
Cu1-N3	1.920(2)	Cu3-N8	1.995(4)
Cu1-N4	1.974(4)	Na1-O5	2.424(4)
Cu2-O4	1.892(3)	Na1-O15	2.459(4)
Cu2-O14	1.910(3)	Na1-O14	2.479(4)
Cu2-N6	1.912(4)	Na1-O4	2.502(4)
Cu2-N2	1.963(4)	Na1-O8	2.586(4)
Cu3-O15	1.891(3)	Na1-O16	2.639(3)
Angles		Angles	
O5-Cu1-O8	85.06(14)	O14-Na1-O4	61.17(11)
O5-Cu1-N3	89.37(15)	O5-Na1-O8	61.37(11)
O8-Cu1-N3	160.27(16)	O15-Na1-O8	114.02(12)
O5-Cu1-N4	161.65(17)	O14-Na1-O8	146.46(15)
O8-Cu1-N4	90.62(16)	O4-Na1-O8	117.95(13)
N3-Cu1-N4	100.21(17)	O5-Na1-O16	113.76(12)
O4-Cu2-O14	83.61(14)	O15-Na1-O16	60.56(11)
O4-Cu2-N6	165.83(17)	O14-Na1-O16	121.70(13)
O14-Cu2-N6	89.81(16)	O4-Na1-O16	156.27(14)
O4-Cu2-N2	88.49(15)	O8-Na1-O16	73.64(11)
O14-Cu2-N2	163.39(17)	O5-Na1-Br4	108.94(11)
N6-Cu2-N2	100.88(17)	O15-Na1-Br4	69.93(9)
O15-Cu3-O16	85.58(14)	O14-Na1-Br4	89.77(10)
O15-Cu3-N7	88.96(15)	O4-Na1-Br4	119.12(11)

Table 2. Cont.

Bond		Bond	
O16-Cu3-N7	160.44(17)	O8-Na1-Br4	60.44(9)
O15-Cu3-N8	159.11(16)	O16-Na1-Br4	84.55(9)
O16-Cu3-N8	91.21(14)	O5-Na1-Br5	69.86(10)
N7-Cu3-N8	100.31(16)	O14-Na1-Br5	129.69(11)
O5-Na1-O15	174.12(13)	O4-Na1-Br5	100.19(10)
O5-Na1-O14	122.79(12)	O8-Na1-Br5	83.81(9)
O15-Na1-O14	63.08(11)	O16-Na1-Br5	58.83(8)
O5-Na1-O4	62.56(11)	Br4-Na1-Br5	135.44(6)
O15-Na1-O4	123.19(13)		

In the crystal structure of the coordination compound **1**, three Cu<sup>II</sup> atoms (Cu1, Cu2, and Cu3) are located in the N<sub>2</sub>O<sub>2</sub> cavities of the deprotonated (HL)<sup>3−</sup> units, the Cu1 and Cu3 atoms are coordinated with two phenoxy atoms and two nitrogen atoms, respectively. The Cu2 atom is coordinated by two nitrogen atoms (N2 and N6) and four oxygen atoms (O2, O4, O14, and O10) from two deprotonated (HL)<sup>3−</sup> units. By means of continuous shape measures (CShM), the configuration of the Cu1 and Cu3 atoms is basically the same, all of which form distorted quadrilateral geometries and the Cu2 atom form a distorted octahedron configuration [84] (Figure 1c). The Na<sup>I</sup> atom is octa-coordinated with the geometry of a distorted hexagonal bipyramid (when the value of CShM is the smallest, the ideal structure is the hexagonal bipyramid configuration), which is coordinated by six oxygen (O4, O5, O8, O14, O15, and O16) atoms and two bromine (Br4 and Br5) atoms from two deprotonated (HL)<sup>3−</sup> units (Figure 1b).

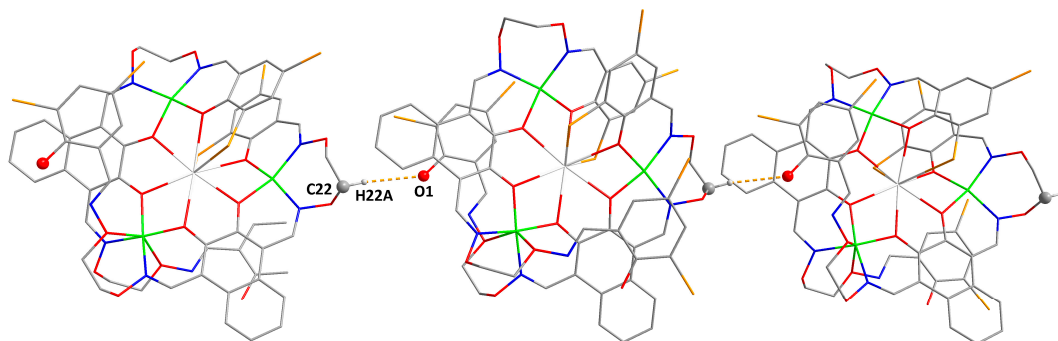
In the crystal structure of the coordination compound **1**, there are three pairs of intramolecular O1-H1B...N1, O9-H9...N5, and C39-H39A...O21 (Figure 2), and a pair of intermolecular C22-H22A...O1 interactions, as summarized in Table 3. The anion picrate was linked to coordination compound molecules through an intermolecular C39-H39A...O21 interaction, making the molecular structure more stable. In addition, a one-dimensional (1D) supramolecular structure was formed by intermolecular C22-H22A...O1 interactions (Figure 3).



**Figure 2.** View of the intramolecular and intermolecular hydrogen bondings of the coordination compound **1** (for clarity purpose, hydrogen atoms are omitted, except those forming hydrogen bonds).

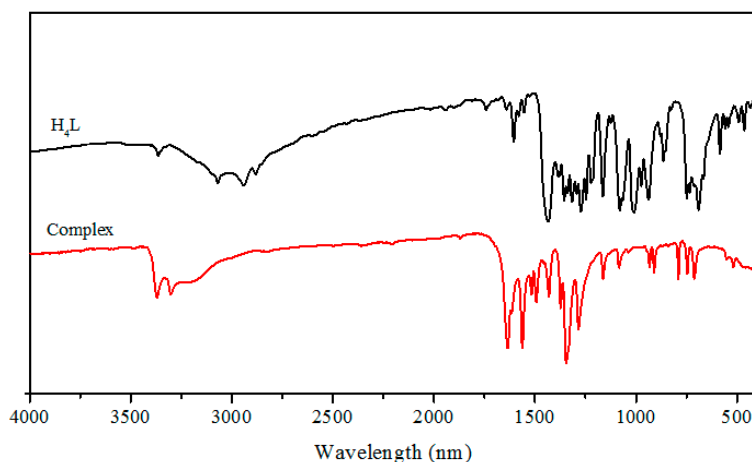
**Table 3.** Hydrogen bonding interactions ( $\text{\AA}$ ,  $^\circ$ ) for the coordination compound **1**.

D-H...A	D-H	H...A	D...A	D-H...A
O1-H1B...N1	0.96	1.80	2.643(6)	144
O9-H9...N5	0.82	1.91	2.632(6)	147
C39-H39A...O21	0.97	2.11	3.014(9)	154
C22-H22A...O1	0.97	2.64	3.601(6)	169

**Figure 3.** The one-dimensional (1D) supramolecular structure of the coordination compound **1** with inter-molecular hydrogen bondings (hydrogen atoms, except those forming hydrogen bonds, are omitted for clarity).

### 3.2. IR Spectra

The FT-IR spectral data of  $H_4L$  and its corresponding  $Cu^{II}-Na^I$  coordination compound showed different bands in the  $400\text{--}4000\text{ cm}^{-1}$  region in Figure 4, and the important bands that are listed in Table 4. The spectrum of the free ligand  $H_4L$  showed a typical O–H stretching band at  $3307\text{ cm}^{-1}$  that belongs to the phenolic hydroxyl group. For the coordination compound **1**, there is a narrow typical O–H stretching band at  $3303\text{ cm}^{-1}$  because of the non-deprotonated phenolic hydroxyl group, and another narrow peak may be the C–H stretching band of the benzene ring. The wide peak at about  $3200\text{ cm}^{-1}$  may be the O–H stretching band in the water. The  $NO_2$  stretching of the picrate anion appeared at about  $1380\text{ cm}^{-1}$  in the coordination compound **1** spectrum. The typical C=N stretching band of the free ligand appeared at  $1605\text{ cm}^{-1}$ . The typical C=N stretching band of the coordination compound **1** appeared at  $1601\text{ cm}^{-1}$  [85]. The Ar–O stretching band of the free ligand appeared at  $1244\text{ cm}^{-1}$ , while that of the coordination compound **1** is observed at  $1215\text{ cm}^{-1}$ , the C=N and Ar–O stretching frequencies are shifted, indicating that the  $Cu^{II}$  atoms are coordinated with the free ligand.

**Figure 4.** Infrared spectra of naphthalenediol-based bis(Salamo)-type ligand ( $H_4L$ ) and its coordination compound.

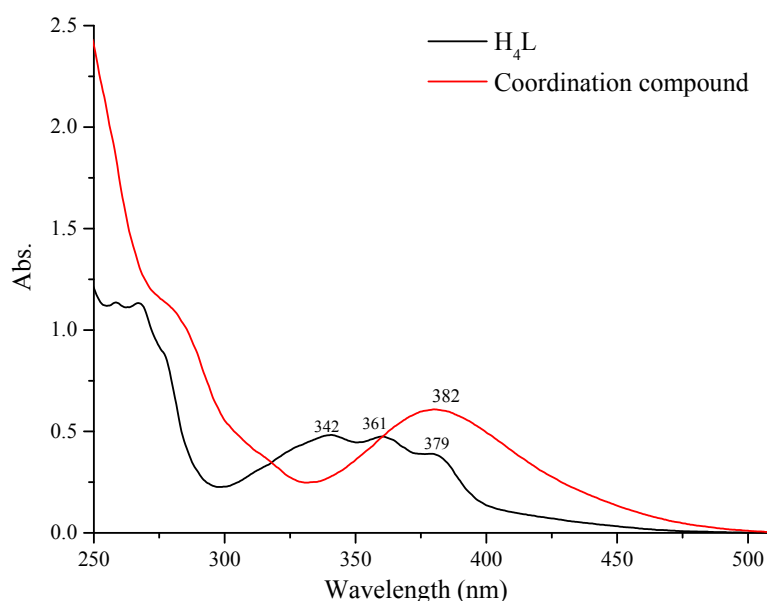


**Table 4.** The major FT-IR data of H<sub>4</sub>L and its Cu<sup>II</sup>-Na<sup>I</sup> coordination compound (cm<sup>−1</sup>).

Compound	$\nu(\text{O-H})$	$\nu(\text{C=N})$	$\nu(\text{Ar-})$
H <sub>4</sub> L	3307	1605	1256
[Cu <sub>3</sub> (HL) <sub>2</sub> Na]·Pic	3303	1601	1215

### 3.3. UV-Vis Spectra

The UV-Vis absorption spectra of the free ligand H<sub>4</sub>L and its corresponding Cu<sup>II</sup>-Na<sup>I</sup> coordination compound in the CHCl<sub>3</sub>/CH<sub>3</sub>OH solution (CHCl<sub>3</sub>/CH<sub>3</sub>OH 3:2 *v/v*, 1.0 × 10<sup>−5</sup> mol/L) are shown in Figure 5. Obviously, the absorption maxima of the ligand H<sub>4</sub>L differ from those of the coordination compound **1**. As shown in Figure 5, for the ligand H<sub>4</sub>L, the peaks at 342 nm ( $\epsilon = 4.8 \times 10^4 \text{ M}^{-1} \cdot \text{cm}^{-1}$ ), 361 nm ( $\epsilon = 4.3 \times 10^4 \text{ M}^{-1} \cdot \text{cm}^{-1}$ ), and 379 nm ( $\epsilon = 3.5 \times 10^4 \text{ M}^{-1} \cdot \text{cm}^{-1}$ ) can be assigned to the intra-ligand  $\pi$ - $\pi^*$  transitions and indicated that the ligand H<sub>4</sub>L contains a large conjugation system. It can be assigned to the  $\pi$ - $\pi^*$  transition of the naphthalene rings [11]. When compared with the free ligand H<sub>4</sub>L, the three absorption peaks disappeared from the UV-vis spectrum of the coordination compound **1**, and one new absorption maxima was observed at ca. 382 nm for the coordination compound **1**, and is assigned to L→M (LMCT) or M→L (MLCT) charge transition which is characteristic of the transition metal coordination compounds with N<sub>2</sub>O<sub>2</sub> coordination sphere [29].

**Figure 5.** The UV-vis spectra of the free ligand H<sub>4</sub>L and its corresponding coordination compound **1**.

### 3.4. Hirshfeld Surface Analysis

The Hirshfeld surfaces [86] of the coordination compound **1** are illustrated in Figure 6, indicating that the surfaces have been mapped over  $d_{\text{norm}}$  and the corresponding location in shape index exists the complementary region of red concave surface surrounded by receptors and the blue convex surface surrounding receptors, further proving that such hydrogen bonding exists. The large and deep red spots on the three-dimensional (3D) Hirshfeld surfaces indicate the close-contact interactions, mainly responsible for the corresponding hydrogen bond contacts. As for the large amount of white region in  $d_{\text{norm}}$  surfaces, it is suggested that there is a weaker and farther contact between molecules, rather than hydrogen bonding. Figure 7 showed that the two-dimensional (2D) plots that were generated [87] correspond to the O⋯H, C⋯H and H⋯H interactions from the Hirshfeld surface of the coordination compound **1**. With the help of these analysis results, different interactions can be

separated from each other that would commonly overlap in full fingerprint plots. The location of H...H interactions appeared at (1.15 Å, 1.20 Å), accounting for 22.4% of the total area of Hirshfeld surfaces. The C...H/H...C interactions in the range of (1.60 Å, 1.12 Å) and appeared as a pair of symmetrical wings, accounting for 6.4% of the total area of Hirshfeld surfaces. The proportion of O...H/H...O interactions occupies 26.3% of the total Hirshfeld surfaces for each molecule of the coordination compound **1**, the contribution of C...C to Hirshfeld surfaces is 0%, indicating that the  $\pi$ - $\pi$  accumulation does not exist. Owing to the existence of weaker hydrogen bonds, the coordination compound can be stable.

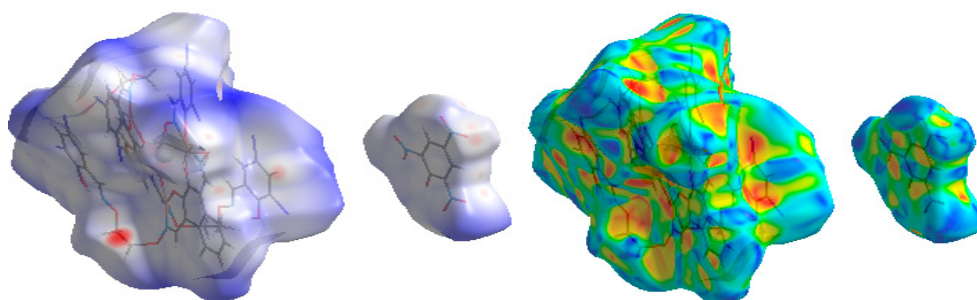


**Figure 6.** Hirshfeld surfaces analysis mapped with  $d_{norm}$  and shape index of the coordination compound **1**.

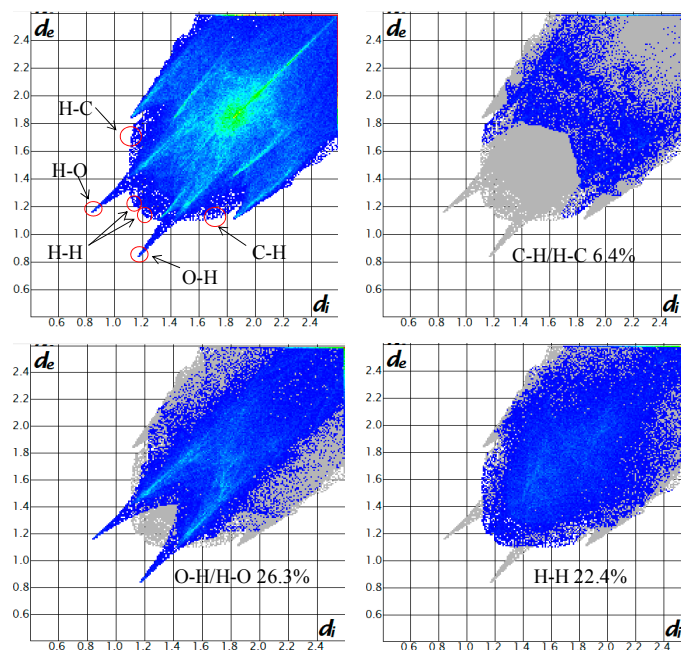


**Figure 7.** Fingerprint plot of the coordination compound **1**: full and resolved into O...H, C...H and H...H contacts showing the percentages of contacts contributed to the total Hirshfeld surface area of molecule.

#### 4. Conclusions

The unexpected hetero-tetranuclear  $\text{Cu}^{\text{II}}\text{-Na}^{\text{I}}$  coordination compound,  $[\text{Cu}_3(\text{HL})_2\text{Na}]\cdot\text{Pic}$  assembly from a naphthalenediol-based bis(Salamo)-type ligand ( $\text{H}_4\text{L}$ ) has been synthesized and characterized. For the central metals, the Cu1 and Cu3 atoms are tetra-coordinated with distorted square geometries, and the Cu2 atoms are hexa-coordinated with a distorted octahedron configuration, while the  $\text{Na}^{\text{I}}$  atom is octa-coordinated with geometry of a distorted hexagonal bipyramid, which is coordinated with six oxygen (O4, O5, O8, O14, O15, and O16) atoms and two bromo (Br4 and Br5)



atoms from two deprotonated (HL)<sup>3−</sup> units. Furthermore, a 1D supramolecular structure was formed by intermolecular C22-H22A⋯O1 interactions. In addition, the Hirshfeld surface analyses indicated that the coordination compound could be stable due to intramolecular hydrogen bonds and some weaker interactions.

**Author Contributions:** W.-K.D. and X.-Y.S. conceived and designed the experiments; L.C. and F.W. performed the experiments; L.-Z.L. analyzed the data; X.-Y.S. contributed reagents/materials/analysis tools; L.-Z.L. and Y.-X.S. wrote the paper.

**Acknowledgments:** The work was financially supported by the National Natural Science Foundation of China (21761018), the Scientific Research Project from Facing Characteristic Discipline of Beijing Union University (KYDE40201703), the Program for Excellent Team of Scientific Research in Lanzhou Jiaotong University (201706) and Beijing Key Laboratory of Bioactive Substances and Functional Foods, Beijing Union University (12213991724010239), which is gratefully acknowledged.

**Conflicts of Interest:** The authors declare no competing financial interests.

## References

1. Chai, L.Q.; Tang, L.J.; Chen, L.C.; Huang, J.J. Structural, spectral, electrochemical and DFT studies of two mononuclear manganese(II) and zinc(II) complexes. *Polyhedron* **2017**, *122*, 228–240. [[CrossRef](#)]
2. Song, X.Q.; Liu, P.P.; Xiao, Z.R.; Li, X.; Liu, Y.A. Four polynuclear complexes based on a versatile salicylamide Salen-like ligand: Synthesis, structural variations and magnetic properties. *Inorg. Chim. Acta* **2015**, *438*, 232–244. [[CrossRef](#)]
3. Wu, H.L.; Pan, G.L.; Bai, Y.C.; Wang, H.; Kong, J. Synthesis, structure, antioxidation, and DNA-binding studies of a binuclear ytterbium(III) complex with bis(*N*-salicylidene)-3-oxapentane-1,5-diamine. *Res. Chem. Intermed.* **2015**, *41*, 3375–3388. [[CrossRef](#)]
4. Zhao, L.; Wang, L.; Sun, Y.X.; Dong, W.K.; Tang, X.L.; Gao, X.H. A supramolecular copper(II) complex bearing Salen-type bisoxime ligand: Synthesis, structural characterization, and thermal property. *Synth. React. Inorg. Met.-Org. Nano-Met. Chem.* **2012**, *42*, 1303–1308. [[CrossRef](#)]
5. Wang, P.; Zhao, L. Synthesis, structure and spectroscopic properties of the trinuclear cobalt(II) and nickel(II) complexes based on 2-hydroxynaphthaldehyde and bis(aminoxoy)alkane. *Spectrochim. Acta Part A* **2015**, *135*, 342–350. [[CrossRef](#)] [[PubMed](#)]
6. Sun, Y.X.; Zhang, Y.J.; Meng, W.S.; Li, X.R.; Lu, R.E. Synthesis and crystal structure of new nickel(II) complex with Salen-type bisoxime ligand. *Asian J. Chem.* **2014**, *26*, 416–418.
7. Sun, Y.X.; Gao, X.H. Synthesis, characterization, and crystal structure of a new Cu<sup>II</sup> complex with Salen-type ligand. *Synth. React. Inorg. Met.-Org. Nano-Met. Chem.* **2011**, *41*, 973–978. [[CrossRef](#)]
8. Sun, Y.X.; Zhao, Y.Y.; Li, C.Y.; Yu, B.; Guo, J.Q.; Li, J. Supramolecular cobalt(II) and copper(II) complexes with schiff base ligand: Syntheses, characterizations and crystal structures. *Chin. J. Inorg. Chem.* **2016**, *32*, 913–920.
9. Li, J.; Zhang, H.J.; Chang, J.; Jia, H.R.; Sun, Y.X.; Huang, Y.Q. Solvent-Induced unsymmetric Salamo-like trinuclear Ni<sup>II</sup> complexes: Syntheses, crystal structures, fluorescent and magnetic properties. *Crystals* **2018**, *8*, 176. [[CrossRef](#)]
10. Chai, L.Q.; Zhang, H.S.; Dong, W.K.; Zhao, Y.L. Synthesis of unsymmetrical ureas with coumarin and thiadiazole ring under microwave irradiation. *Phosphorus Sulfur Silicon* **2010**, *185*, 1332–1337. [[CrossRef](#)]
11. Li, X.Y.; Chen, L.; Gao, L.; Zhang, Y.; Akogun, S.F.; Dong, W.K. Syntheses, crystal structures and catalytic activities of two solvent-induced homotrimeric Co(II) complexes with a naphthalenediol-based bis(Salamo)-type tetraoxime ligand. *RSC Adv.* **2017**, *7*, 35905–35916. [[CrossRef](#)]
12. Li, L.H.; Dong, W.K.; Zhang, Y.; Akogun, S.F.; Xu, L. Syntheses, structures and catecholase activities of homo- and hetero-trinuclear cobalt(II) complexes constructed from an acyclic naphthalenediol-based bis(Salamo)-type ligand. *Appl. Organomet. Chem.* **2017**, *31*, e3818. [[CrossRef](#)]
13. Dias, S.S.; Kirillova, M.V.; Andre, V.; Kirillov, A.M. New tetracopper(II) cubane cores driven by a diamino alcohol: Self-assembly synthesis, structural and topological features, and magnetic and catalytic oxidation properties. *Inorg. Chem.* **2015**, *54*, 5204–5212. [[CrossRef](#)] [[PubMed](#)]
14. Kirillova, M.V.; Kirillov, A.M.; Pombeiro, A.J. Metal-Free and copper-promoted single-pot hydrocarboxylation of cycloalkanes to carboxylic acids in aqueous medium. *Adv. Synth. Catal.* **2009**, *351*, 2936–2948. [[CrossRef](#)]

15. Kirillova, M.V.; Kirillov, A.M.; Kuznetsov, M.L.; Silva, J.A.; Pombeiro, A.J. Alkanes to carboxylic acids in aqueous medium: Metal-free and metal-promoted highly efficient and mild conversions. *Chem. Commun.* **2009**, 2353–2355. [[CrossRef](#)] [[PubMed](#)]
16. Wu, H.L.; Pan, G.L.; Bai, Y.C.; Wang, H.; Kong, J.; Shi, F.; Zhang, Y.H.; Wang, X.L. Preparation, structure, DNA-binding properties, and antioxidant activities of a homodinuclear erbium(III) complex with a pentadentate schiff base ligand. *J. Chem. Res.* **2014**, *38*, 211–217. [[CrossRef](#)]
17. Wu, H.L.; Wang, C.P.; Wang, F.; Peng, H.P.; Zhang, H.; Bai, Y.C. A new manganese(III) complex from bis(5-methylsalicylaldehyde)-3-oxapentane-1,5-diamine: Synthesis, characterization, antioxidant activity and luminescence. *J. Chin. Chem. Soc.* **2015**, *62*, 1028–1034. [[CrossRef](#)]
18. Wu, H.L.; Bai, Y.C.; Zhang, Y.H.; Li, Z.; Wu, M.C.; Chen, C.Y.; Zhang, J.W. Synthesis, crystal structure, antioxidation and DNA-binding properties of a dinuclear copper(II) complex with bis(*N*-salicylidene)-3-oxapentane-1,5-diamine. *J. Coord. Chem.* **2014**, *67*, 3054–3066. [[CrossRef](#)]
19. Chen, C.Y.; Zhang, J.W.; Zhang, Y.H.; Yang, Z.H.; Wu, H.L. Gadolinium(III) and dysprosium(III) complexes with a schiff base bis(*N*-salicylidene)-3-oxapentane-1,5-diamine: Synthesis, characterization, antioxidation, and DNA-binding studies. *J. Coord. Chem.* **2015**, *68*, 1054–1071. [[CrossRef](#)]
20. Wu, H.L.; Bai, Y.C.; Zhang, Y.H.; Pan, G.L.; Kong, J.; Shi, F.R.; Wang, X.L. Two lanthanide(III) complexes based on the schiff base *N*, *N*-Bis(salicylidene)-1,5-diamino-3-oxapentane: Synthesis, characterization, DNA-binding properties, and antioxidation. *Z. Anorg. Allg. Chem.* **2014**, *640*, 2062–2071. [[CrossRef](#)]
21. Wu, H.L.; Pan, G.L.; Wang, H.; Wang, X.L.; Bai, Y.C.; Zhang, Y.H. Study on synthesis, crystal structure, antioxidant and DNA-binding of mono-, di- and poly-nuclear lanthanides complexes with bis(*N*-salicylidene)-3-oxapentane-1,5-diamine. *J. Photochem. Photobiol. B Biol.* **2014**, *135*, 33–43. [[CrossRef](#)] [[PubMed](#)]
22. Li, X.Y.; Kang, Q.P.; Liu, L.Z.; Ma, J.C.; Dong, W.K. Trinuclear Co(II) and mononuclear Ni(II) Salamo-type bisoxime coordination compounds. *Crystals* **2018**, *8*, 43. [[CrossRef](#)]
23. Jia, H.R.; Li, J.; Sun, Y.X.; Guo, J.Q.; Yu, B.; Wen, N.; Xu, L. Two supramolecular cobalt(II) complexes: Syntheses, crystal structures, spectroscopic behaviors, and counter anion effects. *Crystals* **2017**, *7*, 247.
24. Chai, L.Q.; Huang, J.J.; Zhang, J.Y.; Li, Y.X. Two 1-D and 2-D cobalt(II) complexes: Synthesis, crystal structures, spectroscopic and electrochemical properties. *J. Coord. Chem.* **2015**, *68*, 1224–1237. [[CrossRef](#)]
25. Sun, Y.X.; Zhang, S.T.; Ren, Z.L.; Dong, X.Y.; Wang, L. Synthesis, characterization, and crystal structure of a new supramolecular Cd<sup>II</sup> complex with halogen-substituted Salen-type bisoxime. *Synth. React. Inorg. Met.-Org. Nano-Met. Chem.* **2013**, *43*, 995–1000. [[CrossRef](#)]
26. Sun, Y.X.; Xu, L.; Zhao, T.H.; Liu, S.H.; Liu, G.H.; Dong, X.T. Synthesis and crystal structure of a 3D supramolecular copper(II) complex with 1-(3-[(*E*)-3-bromo-5-chloro-2-hydroxybenzylidene]amino)phenyl) ethanone oxime. *Synth. React. Inorg. Met.-Org. Nano-Met. Chem.* **2013**, *43*, 509–513. [[CrossRef](#)]
27. Chai, L.Q.; Zhang, K.Y.; Tang, L.J.; Zhang, J.Y.; Zhang, H.S. Two mono- and dinuclear Ni(II) complexes constructed from quinazoline-type ligands: Synthesis, X-ray structures, spectroscopic, electrochemical, thermal, and antimicrobial studies. *Polyhedron* **2017**, *130*, 100–107. [[CrossRef](#)]
28. Liu, P.P.; Sheng, L.; Song, X.Q.; Xu, W.Y.; Liu, Y.A. Synthesis, structure and magnetic properties of a new one dimensional manganese coordination polymer constructed by a new asymmetrical ligand. *Inorg. Chim. Acta* **2015**, *434*, 252–257. [[CrossRef](#)]
29. Zhao, L.; Dang, X.T.; Chen, Q.; Zhao, J.X.; Wang, L. Synthesis, crystal structure and spectral properties of a 2D supramolecular copper(II) complex with 1-(4-[(*E*)-3-ethoxyl-2-hydroxybenzylidene]amino)phenyl)ethanone oxime. *Synth. React. Inorg. Met.-Org. Nano-Met. Chem.* **2013**, *43*, 1241–1246. [[CrossRef](#)]
30. Zhou, J.J.; Song, X.Q.; Liu, Y.A.; Wang, X.L. Substituent-tuned structure and luminescence sensitizing towards Al<sup>3+</sup> based on phenoxy bridged dinuclear Eu<sup>III</sup> complexes. *RSC Adv.* **2017**, *7*, 25549–25559. [[CrossRef](#)]
31. Jaremko, L.; Kirillov, A.M.; Smoleński, P.; Pombeiro, A.J. Engineering coordination and supramolecular copper-organic networks by aqueous medium self-assembly with 1,3,5-triaza-7-phosphaadamantane (PTA). *Cryst. Growth Des.* **2009**, *9*, 3006–3010. [[CrossRef](#)]
32. Kopylovich, M.N.; Karabach, Y.Y.; Mahmudov, K.T.; Haukka, M.; Pombeiro, A.J. Heterometallic copper(II)-potassium 3D coordination polymers driven by multifunctionalized azo derivatives of  $\beta$ -diketones. *Cryst. Growth Des.* **2011**, *11*, 4247–4252. [[CrossRef](#)]

33. Song, X.Q.; Peng, Y.J.; Chen, G.Q.; Wang, X.R.; Liu, P.P.; Xu, W.Y. Substituted group-directed assembly of Zn(II) coordination complexes based on two new structural related pyrazolone based Salen ligands: Syntheses, structures and fluorescence properties. *Inorg. Chim. Acta* **2015**, *427*, 13–21. [[CrossRef](#)]
34. Chai, L.Q.; Huang, J.J.; Zhang, H.S. An unexpected cobalt (III) complex containing a schiff base ligand: Synthesis, crystal structure, spectroscopic behavior, electrochemical property and SOD-like activity. *Spectrochim. Acta Part A* **2014**, *131*, 526–530. [[CrossRef](#)] [[PubMed](#)]
35. Chai, L.Q.; Wang, G.; Sun, Y.X.; Dong, W.K.; Zhao, L.; Gao, X.H. Synthesis, crystal structure, and fluorescence of an unexpected dialkoxo-bridged dinuclear copper(II) complex with bis(Salen)-type tetraoxime. *J. Coord. Chem.* **2012**, *65*, 1621–1631. [[CrossRef](#)]
36. Chai, L.Q.; Liu, G.; Zhang, Y.L.; Huang, J.J.; Tong, J.F. Synthesis, crystal structure, fluorescence, electrochemical property, and SOD-like activity of an unexpected nickel(II) complex with a quinazoline-type ligand. *J. Coord. Chem.* **2013**, *66*, 3926–3938. [[CrossRef](#)]
37. Song, X.Q.; Liu, P.P.; Liu, Y.A.; Zhou, J.J.; Wang, X.L. Two dodecanuclear heterometallic [Zn<sub>6</sub>Ln<sub>6</sub>] clusters constructed by a multidentate salicylamide Salen-like ligand: Synthesis, structure, luminescence and magnetic properties. *Dalton Trans.* **2016**, *45*, 8154–8163. [[CrossRef](#)] [[PubMed](#)]
38. Song, X.Q.; Cheng, G.Q.; Liu, Y.A. Enhanced Tb(III) luminescence by d<sup>10</sup> transition metal coordination. *Inorg. Chim. Acta* **2016**, *450*, 386–394. [[CrossRef](#)]
39. Wang, L.; Ma, J.C.; Dong, W.K.; Zhu, L.C.; Zhang, Y. A novel self-assembled nickel(II)–cerium(III) heterotetranuclear dimer constructed from N<sub>2</sub>O<sub>2</sub>-type bisoxime and terephthalic acid: Synthesis, structure and photophysical properties. *Z. Anorg. Allg. Chem.* **2016**, *642*, 834–839. [[CrossRef](#)]
40. Peng, Y.D.; Li, X.Y.; Kang, Q.P.; An, G.X.; Zhang, Y.; Dong, W.K. Synthesis and fluorescence properties of asymmetrical Salamo-type tetranuclear zinc(II) complex. *Crystals* **2018**, *8*, 107. [[CrossRef](#)]
41. Dong, W.K.; Wang, Z.K.; Li, G.; Zhao, M.M.; Dong, X.Y.; Liu, S.H. Syntheses, crystal structures, and properties of a Salamo-type tetradentate chelating ligand and its pentacoordinated copper(II) complex. *Z. Anorg. Allg. Chem.* **2013**, *639*, 2263–2268. [[CrossRef](#)]
42. Wang, P.; Zhao, L. An infinite 2D supramolecular cobalt(II) complex based on an asymmetric Salamo-type ligand: Synthesis, crystal structure, and spectral properties. *Synth. React. Inorg. Met.-Org. Nano-Met. Chem.* **2016**, *46*, 1095–1101. [[CrossRef](#)]
43. Dong, W.K.; Ma, J.C.; Dong, Y.J.; Zhao, L.; Zhu, L.C.; Sun, Y.X.; Zhang, Y. Two hetero-trinuclear Zn(II)–M(II) (M = Sr, Ba) complexes based on metallohost of mononuclear Zn(II) complex: Syntheses, structures and fluorescence properties. *J. Coord. Chem.* **2016**, *69*, 3231–3240. [[CrossRef](#)]
44. Dong, X.Y.; Li, X.Y.; Liu, L.Z.; Zhang, H.; Ding, Y.J.; Dong, W.K. Tri- and hexanuclear heterometallic Ni(II)–M(II) (M = Ca, Sr and Ba) bis(Salamo)-type complexes: Synthesis, structure and fluorescence properties. *RSC Adv.* **2017**, *7*, 48394–48403. [[CrossRef](#)]
45. Yang, Y.H.; Hao, J.; Dong, Y.J.; Wang, G. Two zinc(II) complexes constructed from a bis(Salamo)-type tetraoxime ligand: Syntheses, crystal structures and luminescence properties. *Chin. J. Inorg. Chem.* **2017**, *33*, 1280–1292.
46. Dong, W.K.; Ma, J.C.; Zhu, L.C.; Zhang, Y.; Li, X.L. Four new nickel(II) complexes based on an asymmetric Salamo-type ligand: Synthesis, structure, solvent effect and electrochemical property. *Inorg. Chim. Acta* **2016**, *445*, 140–148. [[CrossRef](#)]
47. Akine, S.; Taniguchi, T.; Nabeshima, T. Synthesis and characterization of novel ligands 1,2-bis(salicylideneaminoxyl)ethanes. *Chem. Lett.* **2003**, *30*, 682–683. [[CrossRef](#)]
48. Akine, S.; Taniguchi, T.; Nabeshima, T. Cooperative formation of trinuclear zinc(II) complexes via complexation of a tetradentate oxime chelate ligand, Salamo, and zinc(II) acetate. *Inorg. Chem.* **2004**, *43*, 6142–6144. [[CrossRef](#)] [[PubMed](#)]
49. Akine, S.; Taniguchi, T.; Nabeshima, T. Heterometallic Zn<sub>2</sub>La and ZnLu complexes formed by site-selective transmetalation of a dimeric homotrinuclear Zinc(II) complex. *Chem. Lett.* **2006**, *35*, 604–605. [[CrossRef](#)]
50. Akine, S.; Dong, W.K.; Nabeshima, T. Octanuclear zinc(II) and cobalt(II) clusters produced by cooperative tetrameric assembling of oxime chelate ligands. *Inorg. Chem.* **2006**, *45*, 4677–4684. [[CrossRef](#)] [[PubMed](#)]
51. Akine, S.; Utsuno, F.; Taniguchi, T.; Nabeshima, T. Dinuclear complexes of the N<sub>2</sub>O<sub>2</sub> oxime chelate ligand with zinc(II)–lanthanide(III) as a selective sensitization system for Sm<sup>3+</sup>. *Eur. J. Inorg. Chem.* **2010**, *2010*, 3143–3152. [[CrossRef](#)]

52. Dong, Y.J.; Ma, J.C.; Zhu, L.C.; Dong, W.K.; Zhang, Y. Four 3d–4f heteromultinuclear zinc(II)–lanthanide(III) complexes constructed from a distinct hexadentate  $N_2O_2$ -type ligand: Syntheses, structures and photophysical properties. *J. Coord. Chem.* **2017**, *70*, 103–115. [[CrossRef](#)]
53. Gao, L.; Liu, C.; Wang, F.; Dong, W.K. Tetra-, penta- and hexa-coordinated transition metal complexes constructed from coumarin-containing  $N_2O_2$  ligand. *Crystals* **2018**, *8*, 77. [[CrossRef](#)]
54. Dong, W.K.; Zheng, S.S.; Zhang, J.T.; Zhang, Y.; Sun, Y.X. Luminescent properties of heterotrinnuclear 3d–4f complexes constructed from a naphthalenediol-based acyclic bis(Salamo)-type ligand. *Spectrochim. Acta Part A* **2017**, *184*, 141–150. [[CrossRef](#)] [[PubMed](#)]
55. Dong, X.Y.; Kang, Q.P.; Jin, B.X.; Dong, W.K. A dinuclear nickel(II) complex derived from an asymmetric Salamo-type  $N_2O_2$  chelate ligand: Synthesis, structure and optical properties. *Z. Naturforsch.* **2017**, *72*, 415–420. [[CrossRef](#)]
56. Hao, J.; Liu, L.Z.; Dong, W.K.; Zhang, J.; Zhang, Y. Three multinuclear Co(II), Zn(II) and Cd(II) complexes based on a single-armed Salamo-type bisoxime: Syntheses, structural characterizations and fluorescent properties. *J. Coord. Chem.* **2017**, *70*, 1936–1952. [[CrossRef](#)]
57. Dong, W.K.; Ma, J.C.; Zhu, L.C.; Zhang, Y. Nine self-assembled nickel(II)-lanthanide(III) heterometallic complexes constructed from a Salamo-type bisoxime and bearing N- or O-donor auxiliary ligand: Syntheses, structures and magnetic properties. *New J. Chem.* **2016**, *40*, 6998–7010. [[CrossRef](#)]
58. Hao, J.; Li, L.H.; Zhang, J.T.; Akogun, S.F.; Wang, L.; Dong, W.K. Four homo- and hetero-bimetallic 3d/3d-2s complexes constructed from a naphthalenediol-based acyclic bis(Salamo)-type tetraoxime ligand. *Polyhedron* **2017**, *134*, 1–10. [[CrossRef](#)]
59. Gao, L.; Wang, F.; Zhao, Q.; Zhang, Y.; Dong, W.K. Mononuclear Zn(II) and trinuclear Ni(II) complexes derived from a coumarin-containing  $N_2O_2$  ligand: Syntheses, crystal structures and fluorescence properties. *Polyhedron* **2018**, *139*, 7–16. [[CrossRef](#)]
60. Dong, X.Y.; Akogun, S.F.; Zhou, W.M.; Dong, W.K. Tetranuclear Zn(II) complex based on an asymmetrical Salamo-type chelating ligand: Synthesis, structural characterization, and fluorescence property. *J. Chin. Chem. Soc.* **2017**, *64*, 412–419. [[CrossRef](#)]
61. Zhang, H.; Dong, W.K.; Zhang, Y.; Akogun, S.F. Naphthalenediol-based bis(Salamo)-type homo- and heterotrinnuclear cobalt(II) complexes: Syntheses, structures and magnetic properties. *Polyhedron* **2017**, *133*, 279–293. [[CrossRef](#)]
62. Zheng, S.S.; Dong, W.K.; Zhang, Y.; Chen, L.; Ding, Y.J. Four Salamo-type 3d–4f hetero-bimetallic  $[Zn^{II}Ln^{III}]$  complexes: Syntheses, crystal structures, and luminescent and magnetic properties. *New J. Chem.* **2017**, *41*, 4966–4973. [[CrossRef](#)]
63. Wang, B.J.; Dong, W.K.; Zhang, Y.; Akogun, S.F. A novel relay-sensor for highly sensitive and selective detection of  $Zn^{2+}/Pic^-$  and fluorescence on/off switch response of  $H^+/OH^-$ . *Sens. Actuators B* **2017**, *247*, 254–264. [[CrossRef](#)]
64. Wang, F.; Gao, L.; Zhao, Q.; Zhang, Y.; Dong, W.K.; Ding, Y.J. A highly selective fluorescent chemosensor for  $CN^-$  based on a novel bis(Salamo)-type tetraoxime ligand. *Spectrochim. Acta Part A* **2018**, *190*, 111–115. [[CrossRef](#)] [[PubMed](#)]
65. Dong, W.K.; Akogun, S.F.; Zhang, Y.; Sun, Y.X.; Dong, X.Y. A reversible “turn-on” fluorescent sensor for selective detection of  $Zn^{2+}$ . *Sens. Actuators B* **2017**, *238*, 723–734. [[CrossRef](#)]
66. Wang, L.; Kang, Q.P.; Hao, J.; Zhang, Y.; Bai, Y.; Dong, W.K. Two trinuclear cobalt(II) Salamo-type complexes: Syntheses, crystal structures, solvent effect and fluorescent properties. *Chin. J. Inorg. Chem.* **2018**, *34*, 525–533.
67. Wang, L.; Hao, J.; Zhai, L.X.; Zhang, Y.; Dong, W.K. Synthesis, crystal structure, luminescence, electrochemical and antimicrobial properties of bis(Salamo)-based Co(II) complex. *Crystals* **2017**, *7*, 277. [[CrossRef](#)]
68. Zhang, L.W.; Liu, L.Z.; Wang, F.; Dong, W.K. Unprecedented fluorescent dinuclear  $Co^{II}$  and  $Zn^{II}$  coordination compounds with a symmetric bis(Salamo)-like tetraoxime. *Molecules* **2018**, *23*, 1141. [[CrossRef](#)] [[PubMed](#)]
69. Akine, S.; Taniguchi, T.; Nabeshima, T. Novel synthetic approach to trinuclear 3d-4f complexes: Specific exchange of the central metal of a trinuclear zinc(II) complex of a tetraoxime ligand with a lanthanide(III) ion. *Angew. Chem.* **2002**, *41*, 4670–4673. [[CrossRef](#)] [[PubMed](#)]
70. Akine, S.; Taniguchi, T.; Saiki, T.; Nabeshima, T.  $Ca^{2+}$ - and  $Ba^{2+}$ -selective receptors based on site-selective transmetalation of multinuclear polyoxime-zinc(II) complexes. *J. Am. Chem. Soc.* **2005**, *127*, 540–541. [[CrossRef](#)] [[PubMed](#)]



71. Akine, S.; Takashi, M.; Taniguchi, T.; Saiki, T.; Nabeshima, T. Synthesis, structures, and magnetic properties of tri- and dinuclear copper(II)–gadolinium(III) complexes of linear oligoimine ligands. *Inorg. Chem.* **2005**, *44*, 3270–3274. [[CrossRef](#)] [[PubMed](#)]
72. Akine, S.; Taniguchi, T.; Nabeshima, T. Helical metallohost-guest complexes via site-selective transmetalation of homotrimeric complexes. *J. Am. Chem. Soc.* **2006**, *128*, 15765–15774. [[CrossRef](#)] [[PubMed](#)]
73. Akine, S.; Taniguchi, T.; Nabeshima, T. Acyclic bis( $N_2O_2$  chelate) ligand for trinuclear d-block homo- and heterometal complexes. *Inorg. Chem.* **2008**, *47*, 3255–3264. [[CrossRef](#)] [[PubMed](#)]
74. Chen, L.; Dong, W.K.; Zhang, H.; Zhang, Y.; Sun, Y.X. Structural variation and luminescence properties of triand dinuclear  $Cu^{II}$  and  $Zn^{II}$  complexes constructed from a naphthalenediol-based bis(Salamo)-type ligand. *Cryst. Growth Des.* **2017**, *17*, 3636–3648. [[CrossRef](#)]
75. Sheldrick, G.M. *SHELXS-2016, Program for Crystal Structure Solution*; University of Göttingen: Göttingen Germany, 2016.
76. Sheldrick, G.M. *SHELXL-2016, Program for Crystal Structure Refinement*; University of Göttingen: Göttingen Germany, 2016.
77. Dong, Y.J.; Li, X.L.; Zhang, Y.; Dong, W.K. A highly selective visual and fluorescent sensor for  $Pb^{2+}$  and  $Zn^{2+}$  and crystal structure of  $Cu^{2+}$  complex based-on a novel single-armed Salamo-type bisoxime. *Supramol. Chem.* **2017**, *29*, 518–527. [[CrossRef](#)]
78. Dong, W.K.; Li, X.L.; Wang, L.; Zhang, Y.; Ding, Y.J. A new application of Salamo-type bisoximes: As a relay-sensor for  $Zn^{2+}/Cu^{2+}$  and its novel complexes for successive sensing of  $H^+/OH^-$ . *Sens. Actuators B Chem.* **2016**, *229*, 370–378. [[CrossRef](#)]
79. Akine, S.; Varadi, Z.; Nabeshima, T. Synthesis of planar metal complexes and the stacking abilities of naphthalenediol-based acyclic and macrocyclic Salen-type Ligands. *Eur. J. Inorg. Chem.* **2013**, *35*, 5987–5998. [[CrossRef](#)]
80. Ma, J.C.; Dong, X.Y.; Dong, W.K.; Zhang, Y.; Zhu, L.C.; Zhang, J.T. An unexpected dinuclear Cu(II) complex with a bis(Salamo) chelating ligand: Synthesis, crystal structure, and photophysical properties. *J. Coord. Chem.* **2016**, *69*, 149–159. [[CrossRef](#)]
81. Dong, W.K.; Duan, J.G.; Guan, Y.H.; Shi, J.Y.; Zhao, C.Y. Synthesis, crystal structure and spectroscopic behaviors of Co(II) and Cu(II) complexes with Salen-type bisoxime ligands. *Inorg. Chim. Acta* **2009**, *362*, 1129–1134. [[CrossRef](#)]
82. Akine, S.; Akimoto, A.; Shiga, T.; Oshio, H.; Nabeshima, T. Synthesis, stability, and complexation behavior of isolable Salen-type  $N_2S_2$  and  $N_2SO$  ligands based on thiol and oxime functionalities. *Inorg. Chem.* **2008**, *47*, 875–885. [[CrossRef](#)] [[PubMed](#)]
83. Dong, W.K.; He, X.N.; Yan, H.B.; Lu, Z.W.; Chen, X.; Zhao, C.Y.; Tang, X.L. Synthesis, structural characterization and solvent effect of copper(II) complexes with a variational multidentate Salen-type ligand with bisoxime groups. *Polyhedron* **2009**, *28*, 1419–1428. [[CrossRef](#)]
84. Casanova, D.; Llunell, M.; Alemany, P.; Alvarez, S. The rich stereochemistry of eight-vertex polyhedra: A continuous shape measures study. *Chemistry* **2005**, *11*, 1479–1494. [[CrossRef](#)] [[PubMed](#)]
85. Xu, L.; Zhu, L.C.; Ma, J.C.; Zhang, Y.; Zhang, J.; Dong, W.K. Syntheses, structures and spectral properties of mononuclear  $Cu^{II}$  and dimeric  $Zn^{II}$  complexes based on an asymmetric Salamo-type  $N_2O_2$  ligand. *Z. Anorg. Allg. Chem.* **2015**, *641*, 2520–2524. [[CrossRef](#)]
86. Rohl, A.L.; Moret, M.; Kaminsky, W.; Claborn, K.; McKinnon, J.J.; Kahr, B. Hirshfeld surfaces identify inadequacies in computations of intermolecular interactions in crystals: Pentamorphic 1,8-dihydroxyanthraquinone. *Cryst. Growth Des.* **2012**, *8*, 4517–4525. [[CrossRef](#)]
87. Chattopadhyay, B.; Mukherjee, A.K.; Narendra, N.; Hemantha, H.P.; Sureshbabu, V.V.; Helliwell, M.; Mukherjee, M. Supramolecular architectures in 5,5'-substituted hydantoins: Crystal structures and Hirshfeld surface analyses. *Cryst. Growth Des.* **2010**, *10*, 65–68. [[CrossRef](#)]

